Copyright © 1998, by the International Council of the Aeronautical Sciences (ICAS)
and the American Institute of Aeronautics and Astronautics, Inc.

ICAS-98-4,3,3

A98-31586

Comprehensive Time Analysis in Aeroelastic Simulations

B.J.G. Eussen *
National Aerospace Laboratory
Amsterdam, The Netherlands

M.H.L. Hounjet †
National Aerospace Laboratory
Amsterdam, The Netherlands

M.W. Soijer ‡
Delft University of Technology
Delft, The Netherlands

Abstract: A procedure is presented which yields flutter diagrams using an aeroelastic simulation for a given flight condition, in combination with a parameter analysis for an equivalent linear aeroelastic model.

This equivalent model is constructed by applying the MIMO technique to the time signals obtained from the aeroelastic simulation.

The procedure strongly reduces the amount of nonlinear simulations needed, for instance, at transonic flow conditions, where the linear model can be used as a predictor for the critical flutter boundary of the nonlinear system.

The paper presents the MIMO method and demonstrates its applicability for an aeroelastic testcase.

Introduction

Efficient and reliable prediction of flutter boundaries at nonlinear conditions is an increasingly important aspect of the modern multi-disciplinary aircraft design and analysis process. For such conditions, present for instance at transonic flight, at high angles of attack or in case of structural nonlinearities like backlash, aeroelastic time-marching simulation of the behaviour of the flexible aircraft is a necessary complement to conventional linear methods. Contrary to the latter methods usually operating in the frequency domain, an aeroelastic simulation requires a separate signal analysis procedure to determine frequency and damping information. This procedure is a parameter identification process in which the aeroelastic model is assumed to be linear and a conventional signal analysis procedure is carried out (e.g. Prony fits, ...), like in the analysis of Ground Vibration Tests or Flutter Flight Tests. Disadvantage is that this procedure only yields results in one point of the flutter diagram, and a large number of simulations would be required to obtain sufficient information about the critical flutter boundaries.

As an alternative to the conventional curve-fitting procedures recently a more sophisticated parameter identification process has been developed, which constructs an equivalent linear aeroelastic model having the same properties as the full nonlinear model. This linear model subsequently may be used to obtain complete flutter diagrams in the same way as obtained in conventional flutter analyses, by varying the parameters underlying the identified model, such as dynamic pressure. The parameter identification process underlying the present approach is MIMO. The combination of this process with aeroelastic simulation drastically reduces the computational effort needed at nonlinear conditions and yields a close complement to conventional methods.

The adoption of MIMO-class[1] technology, allows for the possibility to predict the system state at multiple flight conditions from a MIMO identification of a fully-coupled simulation at a single flight condition, by extracting useful data (e.g. Generalized Forces) from the coupled simulation which can be used for other purposes. *

By the aforementioned continuation it is expected to increase efficiency, so that industrial aeroelastic studies might be performed with fully-coupled CFD methods in assessing the critical state cases for a large state space.

The multi-point strategy is explained in Figure 1.

In the present paper the MIMO process is described and its applicability is demonstrated in combination with time-marching aeroelastic simulations.

Stability analysis with time-accurate CFD methods is usually performed with one of the following two strategies:

1. **pk- method (eigenvalue) analysis.** The aerodynamic data required for these methods might be supplied by:
   - i harmonic exitation in time domain which is inefficient when the state space is large.
   - ii time-linearized aerodynamic methods which operate in the frequency domain i.e. for harmonic motions and are known to be limited in frequency especially in the transonic speed regime.

*research scientist
†Senior research scientist
‡Graduate student/research assistant

* *It should be noted that also the analysis might provide a prognostic way to speed up the simulation by allowing for larger time steps*[2]

Copyright © 1998 by ICAS and AIAA. All rights reserved

Copyright © 1998, by the International Council of the Aeronautical Sciences (ICAS)
and the American Institute of Aeronautics and Astronautics, Inc.

iii impuls-response time domain simulation which is prone to noise and is also inefficient when the state space is large.

iv diverging rate method. The latter method is based on linearized form of the equations and is suitable in a design cycle because the turn-around time can be brought back to the minimum. The diverging rate method has been introduced by Hounjet.[3]

2. **Fully-coupled simulation**. This method is especially useful in case of strong nonlinearities and a large number of vibration modes. For a single point the turn-around time is always less than the turn-around time when method 1.i-1.ii are used for the study of a general stability problem. For a restrictive study methods 1.i-1.iv might be more efficient than method 2. It should be mentioned that method 1.iv can be embedded reasonably easy in a time-accurate CFD method.

Experience at NLR has shown that the approach in the k-domain, the s-domain and the time-domain are analogous, as long as the assumption of linearity is not violated and the frequency domain methods have no inherent limitations† which impair the mapping (fitting of generalized forces) between the separate domains.

Therefore the fully-coupled simulation may also be performed using a time integration approach of the generalized forces once adequately fitted in the frequency domain. This eases applications and improves confidence for the coupled simulation if based on linear aerodynamics. ‡ The presentation describes a linear time simulation method and a recent application.

Time signal analysis

As many different time response signals may have to be analyzed a comprehensive set of methods for curve-fitting should be available. In general each time response signal consists of contributions of various modal modes, of which the frequency and damping of each one have to be determined.

Therefore, during an unsteady simulation the data must be analyzed on-line in the time domain in order to determine the behavior of a coupled system. The main purpose of this analysis is to determine the frequency and damping characteristics of the discrete time signal. To fulfil that task the following common SISO approaches might be used[4]):

1. The exponential sine fit,[5]
2. Prony's method,
3. Fast Fourier Transform analysis,
4. Curve-fitting of transfer functions.

Very recently, in a cooporation with TUDelft a feasibility study has been started to apply the promising MIMO-class techniques for that purpose.[4] They will enhance the analysis capability as depicted in Figure 2.

MIMO-class system identification

The adoption of MIMO[1] technology permits a black box § evaluation of the aeroelastic system in such a way that after a single fully-coupled simulation for one flight condition the system state for other flight conditions (e.g. q_{dyn}) might be predicted and to extract useful data (e.g. Generalized Forces) from the coupled simulation which can be used for other purposes.

The main purpose is to extend the single point application of coupled simulation methods to multiple points to make way to postprocessing activities, pk-, k-method etc, based on data extracted from fully-coupled applications.

A 2-DOF example is presented in Figure 3 where we want to assess the transfer functions of the generalized forces from the coupled simulation using only the time trace data. From the coupled responses of x and u at a fixed q_{dyn} the MIMO analyses will deduct the $A, B, C, D, Q_{11}, Q_{12}, Q_{21}$ and Q_{22}. The condition of the system is equivalent to the amount of proportional feedback. A, B, C and D are the system matrices of the elastomechanical system, Q are the tranfer functions of the generalized forces, q_{dyn} the dynamic pressure, x is the elastomechanical state, equivalent to the generalized coordinates and u is the aerodynamic force equivalent to the sum of generalized forces per mode.

The implementation of the MIMO class identification algorithms in the AESIM environment[6] , is aimed at the reduction of the aerodynamic model that operates within the closed loop system of elastomechanical and aerodynamic modes. The closed loop character of the problem results in a requirement for an external reference signal, in order to apply closed loop identification procedures. The complete absence of external noise, as the data at hand is obtained from simulations, and the lack of uncorrelated input signals makes it impossible for any identification procedure to distinguish between elastic and aerodynamic modes.

This problem, together with the low order for which persistency of excitation can be obtained, is pointed out by Hounjet,Eussen and Soijer in.[4] However, identification of the complete, coupled system as a whole is possible in the time domain, resulting in aeroelastic models that describe both elastic and aerodynamic modes. For this purpose, linear regression models are used. In case of the T-tail case as presented in.[4] , a dynamical model is estimated from first and second order differentials. In case of the 3D AGARD standard aeroelastic configuration, a static regression model is used to avoid erroneous modeling of elastomechanical modes.

†due to program inconsistencies

‡Damping and other quantities of interest might be straightforward obtained from the whole aeroelastic system matrix without simulation

§No knowledge is assumed of coefficients of the structural and aerodynamic system

Copyright © 1998, by the International Council of the Aeronautical Sciences (ICAS)
and the American Institute of Aeronautics and Astronautics, Inc.

Decoupled MIMO identification

For the decoupled aerodynamic model as shown in Figure 3, the generalized forces f are expressed in terms of the generalized displacements $d = q$ and speeds $s = \dot{q}$:

$$f_k = \sum_{n=0}^{N-1} (a_n s_{k-n} + b_n d_{k-n}) + \epsilon. \quad (1)$$

In this equation, N is the model order and a and b are the series of regression coefficients. ϵ is the model error. Both the generalized forces and the speeds and displacements are vectors that contain as many rows as there are dynamic modes. This number is called the mode order M. The equation above can be written in matrix form:

$$[f_k] = \begin{bmatrix} A & B \end{bmatrix} \begin{bmatrix} s_k \\ \vdots \\ s_{k-N} \\ d_k \\ \vdots \\ d_{k-N} \end{bmatrix} + \epsilon. \quad (2)$$

The matrices A and B are of size M by MN each. From a time series of experimental data, either from measurements or simulations, the optimal values for the matrices A and B are determined. In order to apply a least-squares estimator, the data for all time points 0 to K are organized columnwise:

$$\begin{bmatrix} f_N & \dots & f_K \end{bmatrix} = \begin{bmatrix} A & B \end{bmatrix} \begin{bmatrix} s_N & \dots & s_K \\ \vdots & & \vdots \\ s_0 & \dots & s_{K-N} \\ d_N & \dots & d_K \\ \vdots & & \vdots \\ d_0 & \dots & d_{K-N} \end{bmatrix} + \epsilon. \quad (3)$$

If the most right-hand matrix of this expression is referred to as X, the optimal regression matrices A and B can be found if the inverse of XX^T exists:

$$\begin{bmatrix} \widehat{A} & \widehat{B} \end{bmatrix} = \begin{bmatrix} f_N & \dots & f_K \end{bmatrix} X^T (XX^T)^{-1}. \quad (4)$$

Note that the existence of the inverse of XX^T can not be guaranteed; the applicability of the method therefore depends on the data set at hand. However, for systems for which all dynamic modes have been excited properly, identifiability of the matrices A and B is readily achieved.

Coupled MIMO identification

Identification of a coupled dynamic model is handled along the same lines as sketched above. The system at hand is an autonomous dynamic system with **no** inputs and two sets of outputs: one for the speeds, and one for the displacements. Since speeds will be introduced in the model automatically as the time derivatives of the displacements, the model is designed to model displacements only. The displacements for each of the M modes are grouped in the vector $x \in R^{M \times L}$.

For the discrete time systems, the zero-order differential is set to be equal to the displacements themselves:

$$\Delta_k^0 = x_k. \quad (5)$$

From this, the higher order differentials are derived:

$$\Delta_k^L = \Delta_{k+L}^0 - \Delta_k^0 = x_{k+L} - x_k \quad (6)$$

$$\Delta_k^2 = \Delta_{k+L}^L - \Delta_k^L = x_{k+2} - 2x_{k+L} + x_k \quad (7)$$

$$\cdot \quad (8)$$

The propagation of displacements in the dynamic system is now expressed in terms of the first order differential:

$$x_{k+L} = x_k + \Delta_k^L. \quad (9)$$

Likewise, the first order differential for each new time step is expressed in the second order differential for the preceding time step:

$$\Delta_{k+L}^L = \Delta_k^L + \Delta_k^2. \quad (10)$$

Finally, the second order differential is modelled as a linear combination of the zero and first order differentials:

$$\Delta_k^2 = A\Delta_k^0 + B\Delta_k^L + \epsilon. \quad (11)$$

The complete system can now be expressed in state-space form, yielding the displacements and first order differentials - hence the speeds - for a new time point. The state vector is a stacked column vector of zero and first order differentials, each of size M by 1:

$$\begin{bmatrix} x \\ \Delta^L \end{bmatrix}_{k+1} = \begin{bmatrix} I & I \\ A & I+B \end{bmatrix} \begin{bmatrix} x \\ \Delta^L \end{bmatrix}_k + \begin{bmatrix} 0 \\ \epsilon \end{bmatrix}. \quad (12)$$

To identify the unknown matrices A and B, the first order differentials for all available time points - excluding the very first - are grouped columnwise to serve as a set of observations for a least-square estimator. The regressors are the stacked displacements and first order differentials for all time points, excluding the very last:

$$\begin{bmatrix} \Delta_2^L & \dots & \Delta_N^L \end{bmatrix} = \begin{bmatrix} A & I+B \end{bmatrix} X + \epsilon \quad (13)$$

Copyright © 1998, by the International Council of the Aeronautical Sciences (ICAS)
and the American Institute of Aeronautics and Astronautics, Inc.

in which

$$X = \begin{bmatrix} x_L & \dots & x_{N-L} \\ \Delta_L^L & \dots & \Delta_{N-L}^L \end{bmatrix} \quad (14)$$

$$X \in R^{2M\times(N-L)}. \quad (15)$$

The optimal matrices A and B in a least-squares sense are found using the pseudo-inverse of X:

$$\begin{bmatrix} \widehat{A} & I+\widehat{B} \end{bmatrix} = \begin{bmatrix} \Delta_2^L & \dots & \Delta_N^L \end{bmatrix} X^T (XX^T)^{-1}. \quad (16)$$

Like for the static system described before, identifiability is dependent on the existence of the matrix inverse of XX^T.

Time-simulation with linear aerodynamics

To ease applications and to build confidence a coupled simulation should also be run based on linear aerodynamics. This requires the generalized forces (transfer functions) which are in general available in the frequency domain to be fitted [7],[8] and transformed to the time-domain.[9] A feasibility study with 2-D airloads and 3-D airloads was performed in.[4]

Time-simulation with linear aerodynamics is performed along the following steps:

- *Padé approximation*

  The assumption is made that the behavior of any unsteady parameter of interest such as an aerodynamic load or a pressure coefficient can be described by an appropriate form for the transfer function which is a ratio of two s dependent polynomials which is known as the Padé approximation:

$$F_{ij}(s) = \frac{A_0^{ij} + A_1^{ij}s + A_2^{ij}s^2 + \dots + A_m^{ij}s^m}{1 + B_1^{ij}s + B_2^{ij}s^2 + \dots + B_n^{ij}s^n} \quad (17)$$

  with:

$$s \equiv d + \jmath k \quad (18)$$

  The complex curve fitting procedure is used also here to obtain the approximation.

- *Partial fractioning*

  In order to obtain a good fit of the generalized forces, the order of the numerator is bound to $m \leq n+2$ and the order of the denominator, n, is set to a maximum of usually 3. This does not imply that every generalized force, F_{ij}, actually has three states. If m is larger then n a partial fractioning has to be performed in order to ease transformation to time domain:

$$F_{ij}(s) = A_0^{ij} + A_1^{ij}s + A_2^{ij}s^2 + \quad (19)$$
$$+ \frac{a_0^{ij} + a_1^{ij}s + \dots + a_{n-1}^{ij}s^{n-1}}{1 + B_1^{ij}s + \dots + B_n^{ij}s^n}$$

- *Transformation to state-space form*

  The rational polynomial, or the residual of the partial fraction, is transformed to state space form:¶

$$F_{ij}(t) = \bar{A}_0^{ij}q_j(t) + \bar{A}_1^{ij}\frac{dq_j}{dt} + \bar{A}_2^{ij}\frac{d^2q_j}{dt^2} +$$
$$+ \begin{pmatrix} c_1^{ij} & c_2^{ij} & c_3^{ij} \end{pmatrix} \begin{pmatrix} x_1^{ij} \\ x_2^{ij} \\ x_3^{ij} \end{pmatrix} + D^{ij}q_j(t) \quad (20)$$

$$\begin{pmatrix} \dot{x}_1^{ij} \\ \dot{x}_2^{ij} \\ \dot{x}_3^{ij} \end{pmatrix} = \begin{pmatrix} 0 & 1 & 0 \\ 0 & 0 & 1 \\ \alpha_1^{ij} & \alpha_2^{ij} & \alpha_3^{ij} \end{pmatrix} \begin{pmatrix} x_1^{ij} \\ x_2^{ij} \\ x_3^{ij} \end{pmatrix}$$
$$+ \begin{pmatrix} 0 \\ 0 \\ 1 \end{pmatrix} q_j(t) \quad (21)$$

$$\alpha_1^{ij} = -\frac{1}{\bar{B}_3^{ij}}$$
$$\alpha_2^{ij} = -\frac{\bar{B}_1^{ij}}{\bar{B}_3^{ij}}$$
$$\alpha_3^{ij} = -\frac{\bar{B}_2^{ij}}{\bar{B}_3^{ij}}$$
$$c_1^{ij} = \frac{a_0^{ij}}{\bar{B}_3^{ij}} - \frac{\bar{a}_3^{ij}}{\bar{B}_3^{ij}}\frac{1}{\bar{B}_3^{ij}}$$
$$c_2^{ij} = \frac{\bar{a}_1^{ij}}{\bar{B}_3^{ij}} - \frac{\bar{a}_3^{ij}}{\bar{B}_3^{ij}}\frac{\bar{B}_1^{ij}}{\bar{B}_3^{ij}}$$
$$c_3^{ij} = \frac{\bar{a}_2^{ij}}{\bar{B}_3^{ij}} - \frac{\bar{a}_3^{ij}}{\bar{B}_3^{ij}}\frac{\bar{B}_2^{ij}}{\bar{B}_3^{ij}}$$
$$D^{ij} = \frac{\bar{a}_3^{ij}}{\bar{B}_3^{ij}}$$

with:

$$\bar{A}_n^{ij} = A_n^{ij}\left(\frac{1}{s_l V\sqrt{\mu}}\right)^n$$
$$\bar{B}_n^{ij} = B_n^{ij}\left(\frac{1}{s_l V\sqrt{\mu}}\right)^n$$
$$\bar{a}_n^{ij} = a_n^{ij}\left(\frac{1}{s_l V\sqrt{\mu}}\right)^n$$

¶The equations are given here for a third order system.

Copyright © 1998, by the International Council of the Aeronautical Sciences (ICAS)
and the American Institute of Aeronautics and Astronautics, Inc.

x is an auxillary vector, s_l is the spatial synchronization factor, V and μ are explained in.[10]

Two- and three-dimensional applications are discussed in[4] where this system is solved using a Newmark scheme.[6]

- *Aeroelastic coupling*

  Coupling of the generalized mass, stiffness and force comes down to a correct assembly of all fitted F_{ij} components into the generalized aeroelastic system equations, see appendix A. The order of the resulting system is unkown, but never exceeds $modes \times (2 + (n \times modes))$.

- *Time Simulation*

  The system, as obtained in appendix A, is solved using a Newmark scheme, for a range of dynamic pressures.

- *Time signal analysis*

  The resulting time signal is analysed using decoupled MIMO identification, as described before. The resulting damping and frequency data are assembled in a flutter diagram, as shown in the section on the three-dimensional application.

Applications

The examples here focus on current ongoing activities with respect to the time-analysis in 3-D. 2-D examples were already presented in.[4]

Three-dimensional application

Calculations have been performed with GUL for the 3-D AGARD standard aeroelastic wing at Mach=0.901. This configuration is described in.[10] Four modes have been selected.

Figure 4 shows a comparison in the frequency domain between the original data (circle) and the fitted data (line-cross) which show a good agreement. More detailed results have been presented in.[4]

Aeroelastic coupling was performed next according to appendix A. The order of the system was 32.

Figure 7 shows a typical result of a subcritical time simulation.

Every time simulation has been analysed using decoupled MIMO identification and the results are shown in Figures 5-6, together with the results of the NLR PK-method using exactly the same generalised force data. In the Figure are also two points representing the frequency and damping values of a fully coupled non-linear full potential AESIM[6] simulation of the wing. All three methods give the same flutter speed. The difference between the linear time simulation and the NLR PK-method is in the damping per mode. The character of the flutter changes from mild (NLR PK-method) to very mild (linear time simulation). Also the non-linear full potential simulations indicate a very mild character close to the flutter point. The symbols in this figure are explained in Table 1.

MIMO-class application

The applicability of the MIMO method[1] in flutter analysis has also been presented in[4] for an aeroelastic investigation which was conducted for one of the 3-D AGARD standard aeroelastic configurations in subsonic and transonic flow. This configuration is described in.[10] The configuration for dynamic response I wing 445.6 model "weakened no. 3" was selected at Mach=0.901. The data were obtained from.[2] This section summarizes the results obtained in[4] with the decoupled method.

Figure 8 shows the generalized forces as obtained from simulation with the identified decoupled MIMO model, together with the original data. The data is plotted for time points after the transition has damped out. An excellent agreement is shown between both datasets (they coincide entirely).

A slightly different decoupled model structure MIMO*, including auto regressive terms on the outputs, leads to slightly larger errors for the same simulation, as shown in Figure 9.

Figure 10 shows recent results of a regression model, with model order one resulting in a static model decoupled $MIMO^0$that does not use any information from the time history. Errors below 10% are achieved for all modes.

Figures 11 and 12 and show results of the the main purpose of the excercise. We increase the airspeed to a supercritical value and apply the MIMO results obtained from fitting the subcritical airspeed data and make the comparison with results of the aeroelastic simulation at the higher airspeed. The linear MIMO model prediction performs very well for the lower 3 modes. Mode 4 is overpredicted. The modified model MIMO* results in smaller errors than the model from the original model set. Results of $MIMO^0$ have yet to be investigated to decide which of the model results in the best estimates for aerodynamic modeling in aeroelastical closed-loop systems.

Conclusions

In this paper aspects of time-analysis in aeroelasticity have been discussed.

The formulation of the MIMO identification procedure has been presented.

The formulation for dynamic coupling with linear aerodynamics has been presented.

Experience with recent applications and ongoing developments led to the following observations:

- The procedure for utilization of linear aerodynamics from the frequency domain to the time domain have been applied with good results.
- Excellent analysis of time signals can be carried out with the coupled MIMO-class procedures.
- The decoupled MIMO-class analysis applications have shown good promise for increasing the **efficiency** of

Copyright © 1998, by the International Council of the Aeronautical Sciences (ICAS)
and the American Institute of Aeronautics and Astronautics, Inc.

coupled simulations by allowing results made for a single flight condition being extented to multiple flight conditions.

Appendix A: Coupled Aeroelastic system

The definition of the structural system is described below.

The generalised coordinates q^i for each vibration mode may be different in time and are based on the generalized modal deflection approach.

The dynamic deformations are expressed in generalized coordinates q^i and their associated modal mass M, damping D, stiffness K and vibration modes $\vec{h}^i$ for N^h modes which satisfy the equation:

$$[M]\frac{d^2q}{d\tau^2} + [D]\frac{dq}{d\tau} + [K]q = \Delta F \tag{22}$$

τ is non-dimensional time.

Equation (22) is transformed to first order:

$$d\frac{\partial Q}{\partial \tau} + kQ = fQ, \tag{23}$$

where $Q = \begin{pmatrix} q_j \\ \vdots \\ q_n \\ \frac{\partial q}{\partial \tau}_j \\ \vdots \\ \frac{\partial q}{\partial \tau}_n \\ x_1^{ij} \\ \vdots \\ x_n^{ij} \\ \vdots \\ x_n^{NN} \end{pmatrix}$,

$$f = \begin{pmatrix}
0 & 0 & 0 & 0 & 0 & 0 & 0 & 0 \\
0 & 0 & 0 & 0 & 0 & 0 & 0 & 0 \\
\Delta D^{11} & \Delta D^{12} & 0 & 0 & \Delta c_1^{11} & \cdots & \Delta c_{n_{11}}^{11} & \Delta c_1^{12} \\
\Delta D^{21} & \Delta D^{22} & 0 & 0 & 0 & 0 & 0 & 0 \\
0 & 0 & 0 & 0 & 0 & 1 & 0 & 0 \\
0 & 0 & 0 & 0 & 0 & 0 & 1 & 0 \\
1 & 0 & 0 & 0 & \alpha_1^{11} & \cdots & \alpha_{n_{11}}^{11} & 0 \\
0 & 0 & 0 & 0 & 0 & 0 & 0 & 0 \\
0 & 0 & 0 & 0 & 0 & 0 & 0 & 0 \\
0 & 1 & 0 & 0 & 0 & 0 & 0 & \alpha_1^{12} \\
0 & 0 & 0 & 0 & 0 & 0 & 0 & 0 \\
0 & 0 & 0 & 0 & 0 & 0 & 0 & 0 \\
1 & 0 & 0 & 0 & 0 & 0 & 0 & 0 \\
0 & 0 & 0 & 0 & 0 & 0 & 0 & 0 \\
0 & 0 & 0 & 0 & 0 & 0 & 0 & 0 \\
0 & 1 & 0 & 0 & 0 & 0 & 0 & 0 \\
0 & 0 & 0 & 0 & 0 & 0 & 0 & 0 \\
\cdots & \Delta c_{n_{12}}^{12} & 0 & 0 & 0 & 0 & 0 & 0 \\
0 & 0 & \Delta c_1^{12} & \cdots & \Delta c_{n_{21}}^{21} & \Delta c_1^{22} & \cdots & \Delta c_{n_{22}}^{22} \\
0 & 0 & 0 & 0 & 0 & 0 & 0 & 0 \\
0 & 0 & 0 & 0 & 0 & 0 & 0 & 0 \\
0 & 0 & 0 & 0 & 0 & 0 & 0 & 0 \\
1 & 0 & 0 & 0 & 0 & 0 & 0 & 0 \\
0 & 1 & 0 & 0 & 0 & 0 & 0 & 0 \\
\cdots & \alpha_{n_{12}}^{12} & 0 & 0 & 0 & 0 & 0 & 0 \\
0 & 0 & 0 & 1 & 0 & 0 & 0 & 0 \\
0 & 0 & 0 & 0 & 1 & 0 & 0 & 0 \\
0 & 0 & \alpha_1^{21} & \cdots & \alpha_{n_{21}}^{21} & 0 & 0 & 0 \\
0 & 0 & 0 & 0 & 0 & 0 & 1 & 0 \\
0 & 0 & 0 & 0 & 0 & 0 & 0 & 1 \\
0 & 0 & 0 & 0 & 0 & \alpha_1^{22} & \cdots & \alpha_{n_{22}}^{22}
\end{pmatrix}$$

$$, \; d = \begin{pmatrix}
1 & 0 & 0 & 0 & 0 & \cdots & 0 \\
0 & 1 & 0 & 0 & 0 & \cdots & 0 \\
0 & 0 & M_{11} - \Delta\bar{A}_2^{11} & M_{12} - \Delta\bar{A}_2^{12} & 0 & \cdots & 0 \\
0 & 0 & M_{21} - \Delta\bar{A}_2^{21} & M_{22} - \Delta\bar{A}_2^{22} & 0 & \cdots & 0 \\
0 & 0 & 0 & 0 & 1 & \cdots & 0 \\
\vdots & \vdots & \vdots & \vdots & \vdots & \ddots & \vdots \\
0 & 0 & 0 & 0 & 0 & \cdots & 1
\end{pmatrix}$$

and

$$k = \begin{pmatrix}
0 & 0 & -1 & 0 & 0 & \cdots & 0 \\
0 & 0 & 0 & -1 & 0 & \cdots & 0 \\
K_{11} - \Delta\bar{A}_0^{11} & K_{12} - \Delta\bar{A}_0^{21} & B_{11} - \Delta\bar{A}_1^{11} & B_{12} - \Delta\bar{A}_1^{12} & 0 & \cdots & 0 \\
K_{21} - \Delta\bar{A}_0^{21} & K_{22} - \Delta\bar{A}_0^{22} & B_{21} - \Delta\bar{A}_1^{21} & B_{22} - \Delta\bar{A}_1^{22} & 0 & \cdots & 0 \\
0 & 0 & 0 & 0 & 0 & \cdots & 0 \\
\vdots & \vdots & \vdots & \vdots & \vdots & \ddots & \vdots \\
0 & 0 & 0 & 0 & 0 & \cdots & 0
\end{pmatrix}. \tag{24}$$

$$\Delta \equiv \frac{1}{s_l{}^3}V^2 \tag{25}$$

$$\frac{\partial Q}{\partial \tau} = d^{-1}\left(f - k\right)Q. \tag{26}$$

References

[1] M.W. Soijer , *Frequency Domain Identification of Rotorcraft State Space Models and Applications to a BO105 Rigid Body Model* Master's thesis, Delft University of Technology, Faculty of Aerospace Engineering, December 1996

[2] B.B. Prananta and M.H.L. Hounjet, *Large time step aero-structural coupling procedures for aeroelastic simulation* . In Proceedings CEAS Symposium: International Forum on Aerelasticity and Structural Dynamics, CEAS, Rome, June 17-20 1997

Copyright © 1998, by the International Council of the Aeronautical Sciences (ICAS)
and the American Institute of Aeronautics and Astronautics, Inc.

[3] M. H. L. Hounjet .*Application of diverging motions to calculate loads for oscillating motions*, AIAA Journal, Vol. 24, No. 10, October 1986, pp 1723-1725 also as *How to make your aerodynamics in flutter calculations cheaper*, NLR MP 85056 U, August 1985.

[4] M.H.L. Hounjet and B.J.G. Eussen and M. Soijer, *Analysis of aeroelastic simulations by fitting time signals*, Proceedings of 1997 CEAS International Forum on Aeroelasticity and Structural Dynamics, Rome, Volume 3, June 1997.

[5] Bennett, Robert M. and Desmarais, Robert N. *Curve Fitting of Aeroelastic Transient Response Data with Exponential Functions*, NASA SP-415

[6] M.H.L. Hounjet and B.J.G. Eussen, *Outline and Application of the NLR Aeroelastic Simulation Method*, ICAS-94-5.8.2, September 1994

[7] M. H. L. Hounjet and B. J. G. Eussen.*Beyond the frequency limit of time-linearized methods*, NLR TP91216 U, June 1991.

[8] M.H.L. Hounjet and B.J.G. Eussen , *Prospects of time-linearized unsteady calculation methods for exponentially diverging motions in aeroelasticity* AIAA paper 92-2122, April 1992

[9] Edwards, J.W. *Unsteady aerodynamic modeling and active aeroelastic control* NASA CR-148019

[10] Yates, C. *AGARD Standard Aeroelastic Configurations for Dynamic Response I-Wing 445.6*, AGARD Report No. 765, 1988.

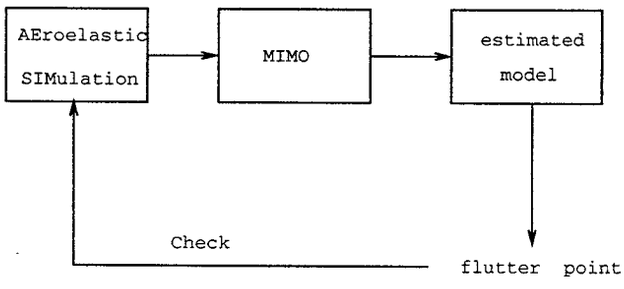

Figure 1: Flowdiagram multi-point strategy.

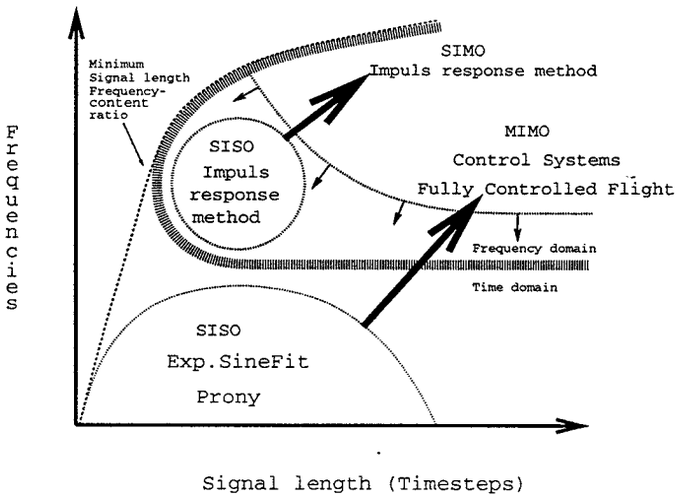

Figure 2: Deployment time-analysis methods with respect to aeroelastic sytems

mode	NLR PK	Lin. time Sim.	AESIM
1	+	----	o-o
2	*	...	o-o
3	x	-.-.	o-o
4	o	- - - -	o-o

Table 1: Symbols in Figure 5-6

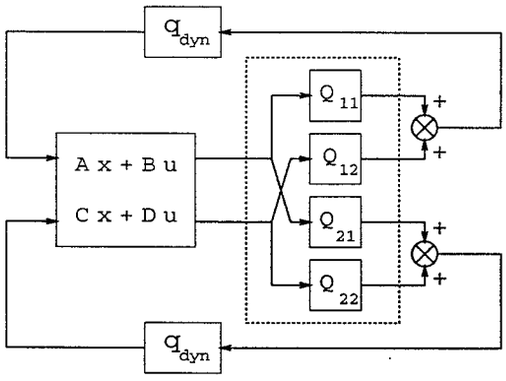

Figure 3: Generic 2 mode aeroelastic system

Copyright © 1998, by the International Council of the Aeronautical Sciences (ICAS)
and the American Institute of Aeronautics and Astronautics, Inc.

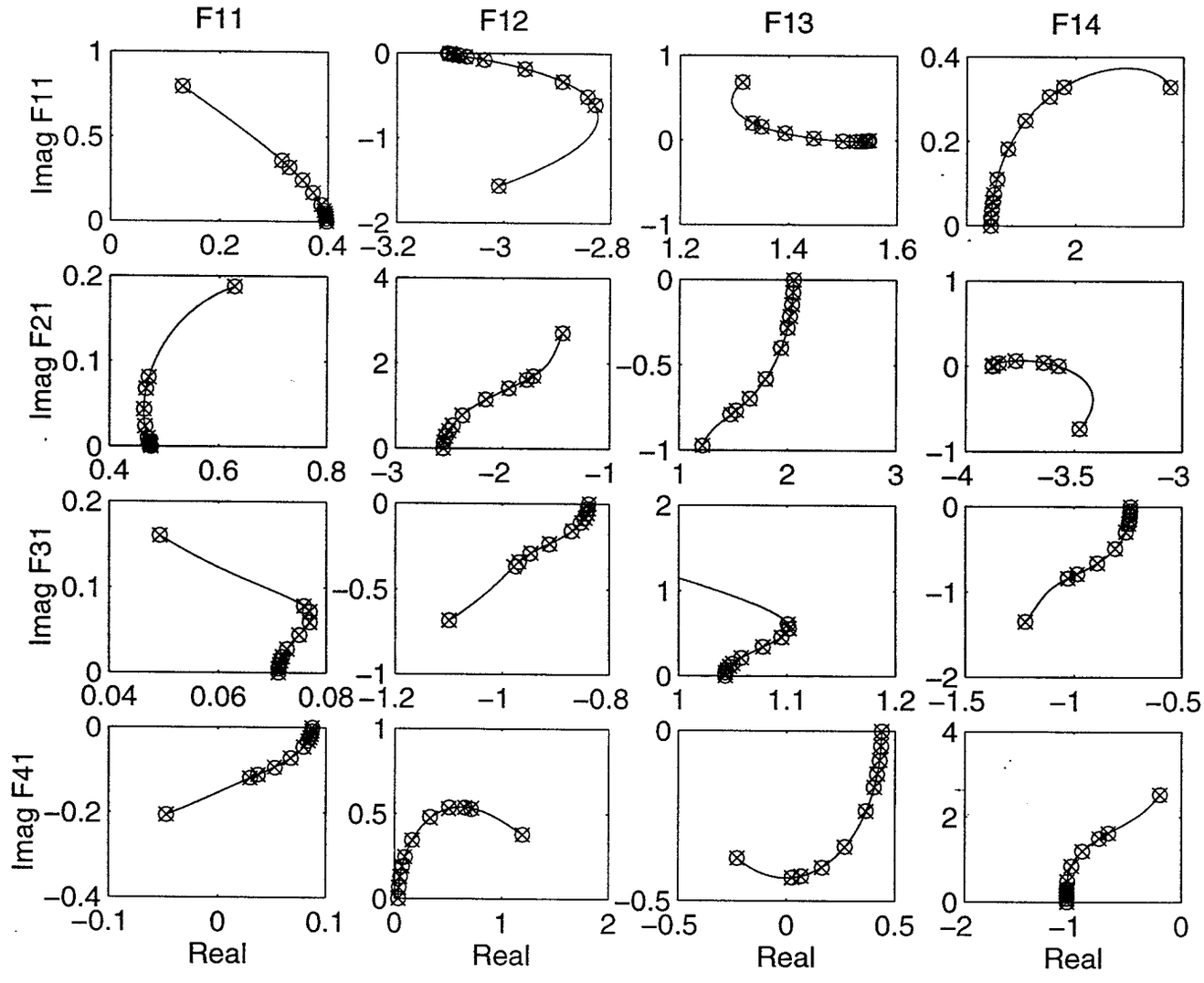

Figure 4: Comparison of directly calculated (o) and fitted (x) generalized forces for the first four modes of AGARD wing 445.6 at M_∞=0.901

Copyright © 1998, by the International Council of the Aeronautical Sciences (ICAS)
and the American Institute of Aeronautics and Astronautics, Inc.

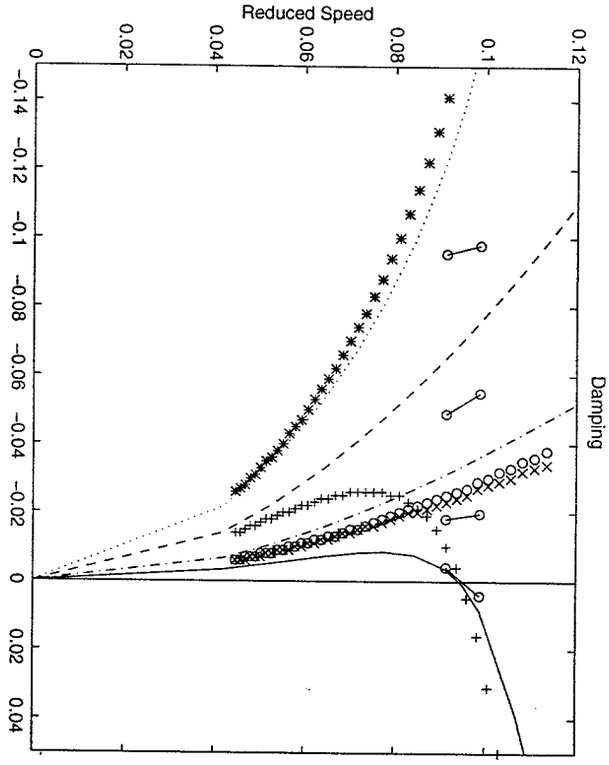

Figure 5: Comparison of damping versus reduced speed

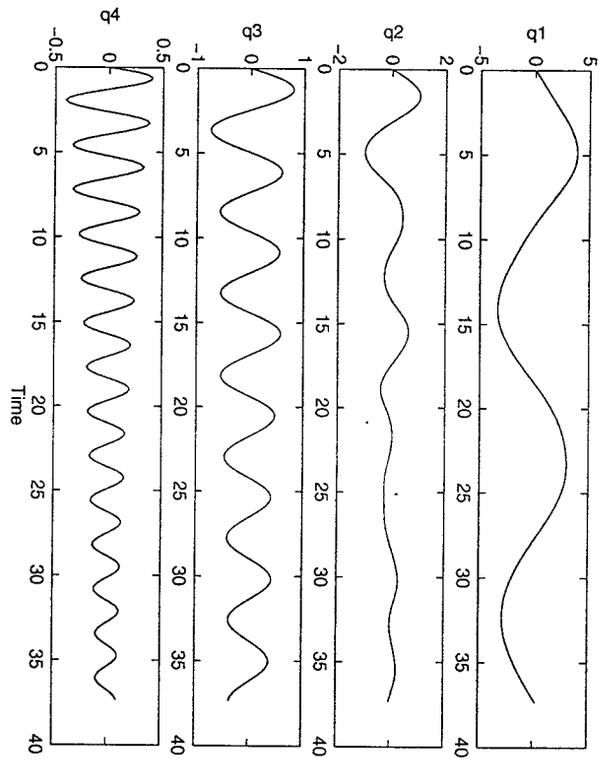

Figure 7: Time response of linear time simulation in subcritical condition

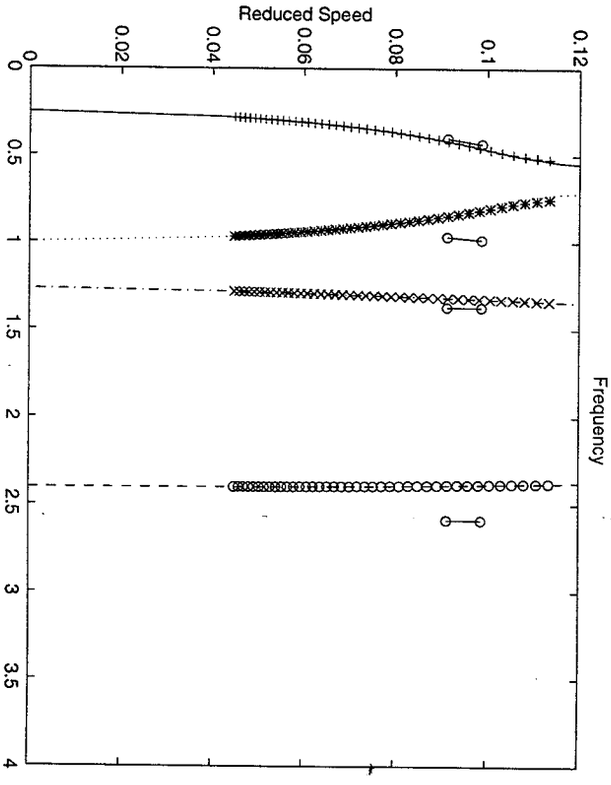

Figure 6: Comparison of frequency versus reduced speed

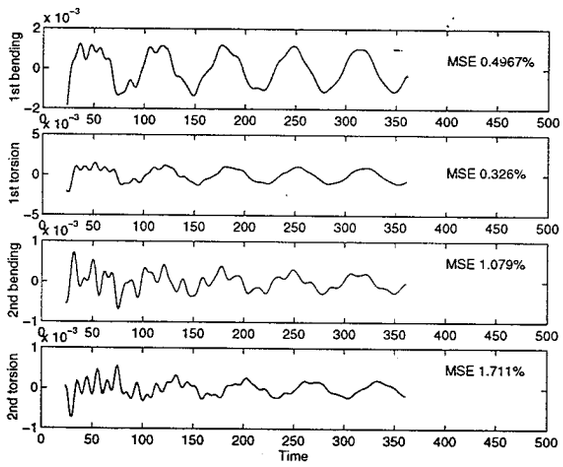

Figure 8: Comparison of decoupled MIMO fitted (...) and original (-) generalized forces data for AGARD aeroelastic system at subcritical flight condition

Copyright © 1998, by the International Council of the Aeronautical Sciences (ICAS)
and the American Institute of Aeronautics and Astronautics, Inc.

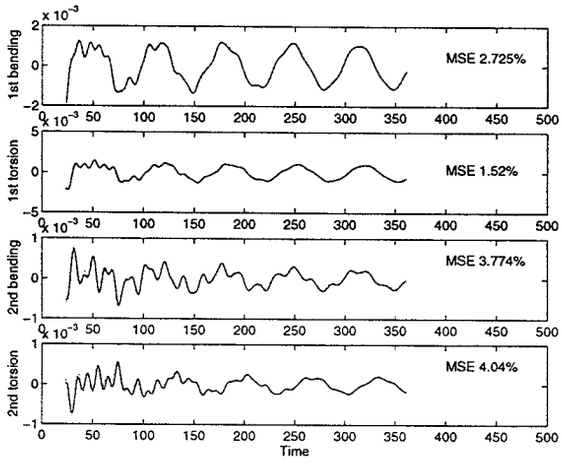

Figure 9: Comparison of decoupled MIMO* fitted (...) with auto regressive terms on outputs and original (-) generalized forces data for AGARD aeroelastic system at subcritical flight condition

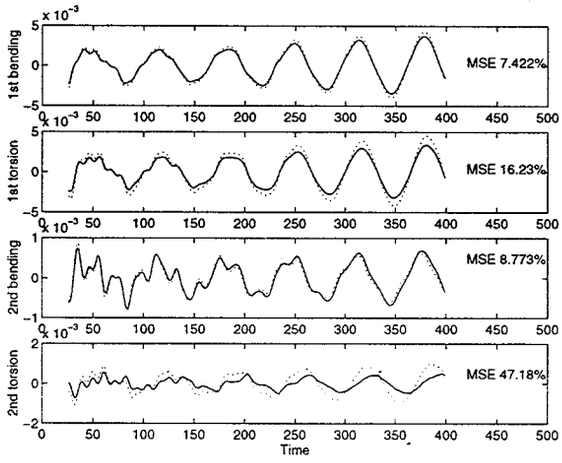

Figure 11: Comparison of MIMO **predicted** (...) and reference (-) generalized forces data for AGARD aeroelastic system at supercritical flight condition

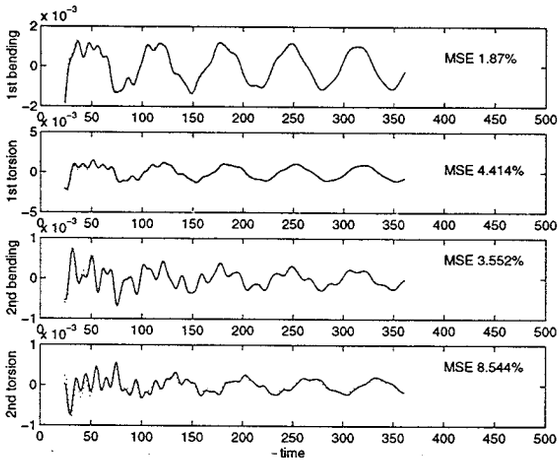

Figure 10: Comparison of $MIMO^0$ fitted (...) with regressive terms on outputs and original (-) generalized forces data for AGARD aeroelastic system at subcritical flight condition

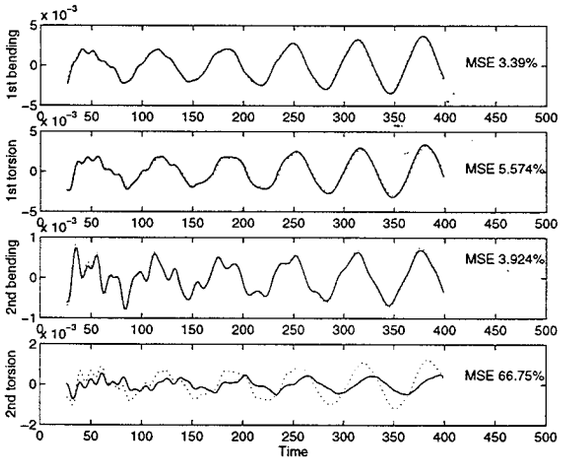

Figure 12: Comparison of MIMO* **predicted** (...) and reference (-) generalized forces data for AGARD aeroelastic system at supercritical flight condition